Journal of Luminescence 203 (2018) 616–628

Contents lists available at ScienceDirect

Journal of Luminescence

journal homepage: www.elsevier.com/locate/jlumin

Spectroscopic and molecular docking studies of the binding of the angiotensin II receptor blockers (ARBs) azilsartan, eprosartan and olmesartan to bovine serum albumin

Amer M. Alanazi[a], Ali S. Abdelhameed[a,*], Ahmed H. Bakheit[a], Eman S.G. Hassan[b], Maha S. Almutairi[a], Hany W. Darwish[a,c], Mohamed I. Attia[a,d]

[a] King Saud University, Department of Pharmaceutical Chemistry, College of Pharmacy, P.O. Box 2457, Riyadh 11451, Saudi Arabia
[b] Developmental Pharmacology Department, National Organization for Drug Control and Research, Cairo, Egypt
[c] Department of Analytical Chemistry, Faculty of Pharmacy, Cairo University, Kasr El-Aini Street, ET 11562 Cairo , Egypt
[d] Medicinal and Pharmaceutical Chemistry Department, Pharmaceutical and Drug Industries Research Division, National Research Centre, Dokki, Giza 12622, Egypt

ARTICLE INFO

Keywords:
Azilsartan
Eprosartan
Olmesartan
Fluorescence spectroscopy
Molecular docking

ABSTRACT

Angiotensin receptor blockers (ARBs) represent a group of widely used therapeutic agents for the effective control of hypertension and other cardiovascular problems. Herein, the interactions of three important members of the ARBs (azilsartan, eprosartan and olmesartan) with bovine serum albumin (BSA) have been explored employing a set of simple spectroscopic approaches complemented with molecular docking studies. Steady state fluorescence emission results demonstrated the ARBs-induced quenching of the intrinsic fluorescence of BSA, which turned out to be a result of the formation of non-fluorescent complexes. The determined Stern-Volmer and binding constants were in the 10^4 magnitude, which were declined with the increase in temperature that primarily indicated static type of quenching. Subsequent analysis of the fluorescence data to explore the thermodynamic characteristics of these interactions showed spontaneous reactions with negative ΔH° values and positive ΔS° values, which suggest the involvement of electrostatic binding forces along with hydrogen bonding. Competitive binding studies were conducted with the aid of known BSA site markers to find the binding region of BSA for the investigated ligands. This was further supported by molecular docking simulations that ascertained the efficient binding of the three ligands to Sudlow site I (subdomain IIA) in the BSA structure.

1. Introduction

In a recent report by the American Heart Association [1], an estimate of more than 75% of the population over 40 years of age are living with increased blood pressure. Hypertension is a principal cause of death globally; it is a main risk factor for heart attack, stroke, chronic heart failure, and kidney disease [2]. Owing to their potency in lowering cardiovascular diseases, angiotensin receptor blockers (ARBs) alone or in combination are regarded as first line of treatment for hypertension even in patients with other serious illnesses e.g. heart failure, diabetes, etc. [3]. It was earlier reported that ARBs show high affinity levels to plasma proteins (95–99.5%) [4] which in turn may suggest that such protein binding can alter their activity either by increasing duration of action or reducing the free drug concentration their site of action, hence delaying the time of onset. A number of eight members of the ARBs family are available in the market, they share the main feature of selectively binding to the angiotensin II AT_1 receptor, a receptor that is ubiquitously situated on most tissues throughout the entire body [5]. An important member of the ARBs family is azilsartan medoxomil, which is a prodrug that is hydrolyzed in the gastrointestinal tract to its active moiety, azilsartan. Azilsartan (AZL, Fig. 1a) is a selective blocker of the angiotensin II type 1 receptor (AT1) that stops its binding, causing vasodilatation and decline in the aldosterone effects [6]. AZL was not only shown to have antihypertensive effect but also been claimed to possess reno-protective capabilities *viz* lowering proteinuria, albuminuria, and nephrinuria [7]. Eprosartan (EPR, Fig. 1b), is another selective angiotensin II receptor antagonist with a high affinity for AT1 [8]. Through its angiotensin-II blocking activity, EPR inhibits the angiotensin-II induced vasoconstriction and blocks the angiotensin II -induced stimulation of aldosterone synthesis and secretion by the adrenal cortex, cardiac contraction, renal re-sorption of sodium hence, causes decline in blood pressure [9,10]. Olmesartan

* Corresponding author.
E-mail address: asaber@ksu.edu.sa (A.S. Abdelhameed).

https://doi.org/10.1016/j.jlumin.2018.06.085
Received 9 April 2018; Received in revised form 24 May 2018; Accepted 30 June 2018
Available online 02 July 2018

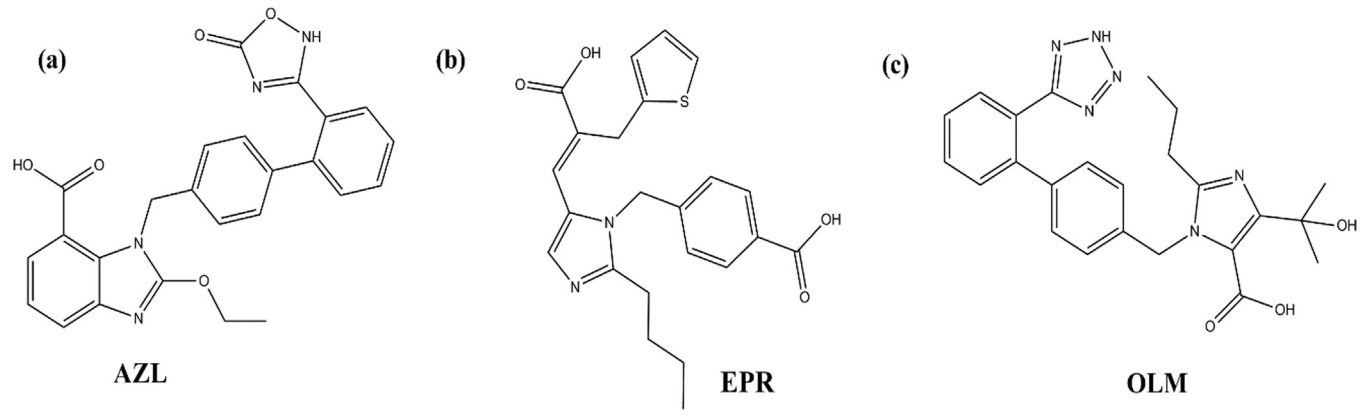

Fig. 1. Chemical structures of AZL, EPR and OLM.

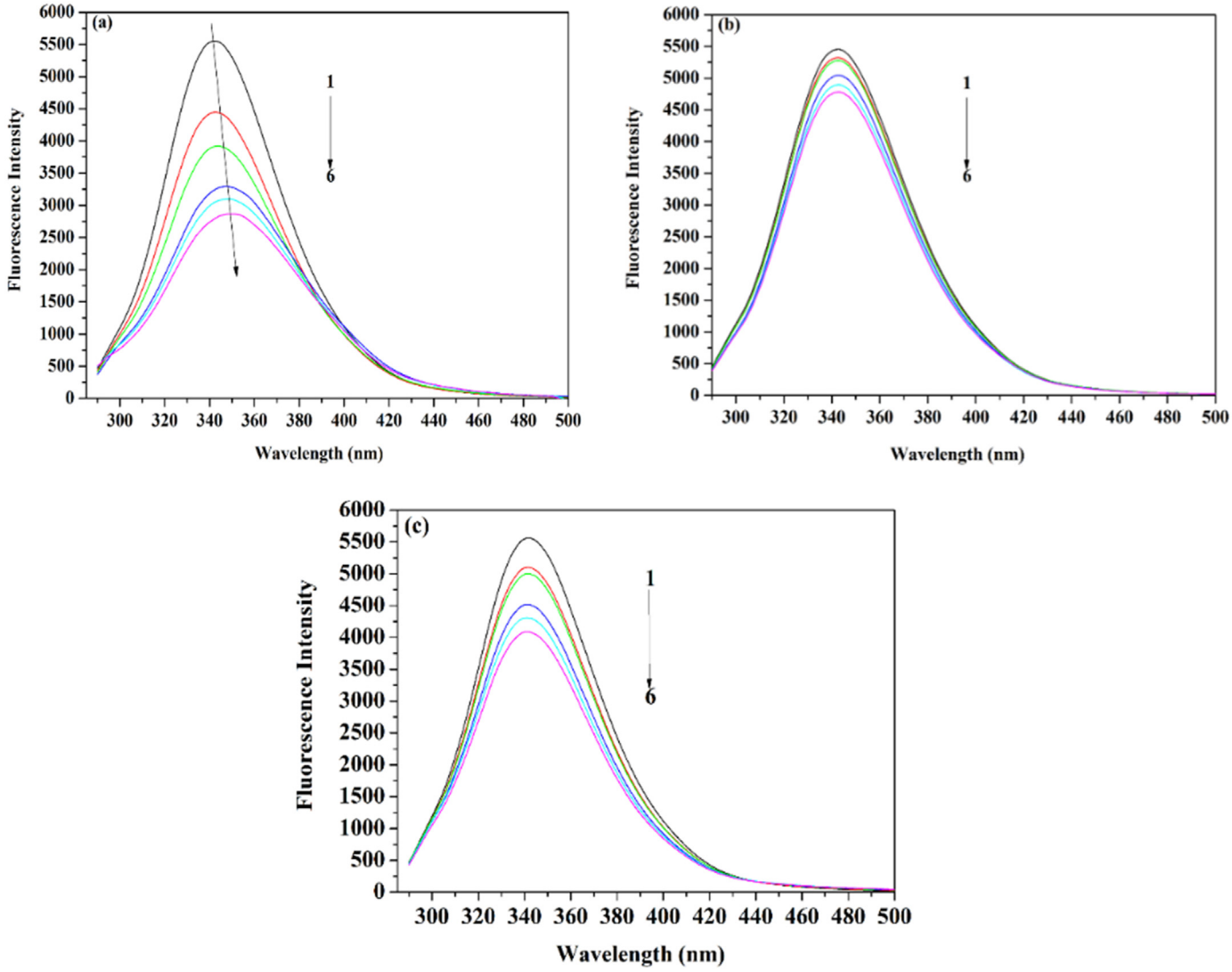

Fig. 2. Representative emission spectra at 298 K showing λ_{em} maxima at 342 nm of BSA (1.5 μM in PBS) in presence of **(a)** AZL (0, 1.5, 3.0, 6.0, 9.0 and 12.0 μM as 1–6) **(b)** EPR (0, 1.5, 3.0, 6.0, 8.0 and 10 μM as 1–6) **(c)** OLM (0, 1.25, 2.5, 5.0, 7.5 and 10 μM as 1–6).

(OLM, Fig. 1c), is a third member of the ARBs family with high potency and selectivity towards blocking the angiotensin AT1 receptor [11]. The drug is also available with medoxomil ester moiety, which is cleaved rapidly by the endogenous esterase releasing the active olmesartan [12].

Pharmacokinetic features of the various drugs represent complicated mechanisms inside the body, which are greatly influenced by the affinity of such drugs to either the plasma constituents and/or the different tissues [13,14]. Former reports have shown various promising synthesized compounds have failed and lost their way to the clinical use

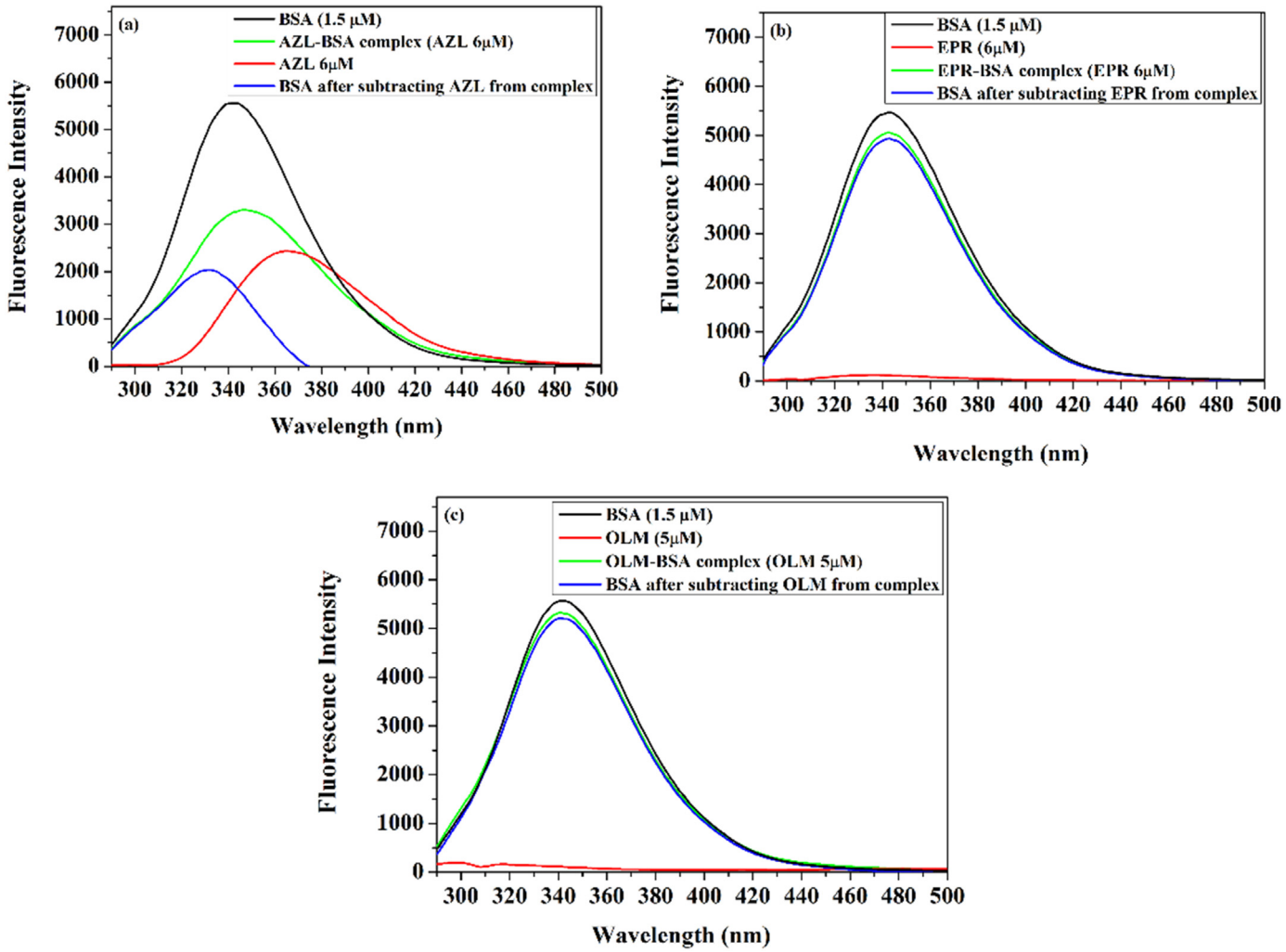

Fig. 3. Fluorescence emission spectra at 298 K showing λ_{em} peaks of BSA (1.5 μM in PBS) and standards of **(a)** AZL (6.0 μM) **(b)** EPR (6.0 μM) **(c)** OLM (5.0 μM) along with their respective BSA-complexes and subtracted spectra from BSA-complexes.

because of their binding failure to circulating proteins [15–17]. This in fact have made the binding of drugs to the circulating proteins an important requirement during drug development [18]. Such circulating proteins include albumin, lipoproteins, globulins, and acid glycoproteins. Precisely, the unbound (free) drug amount circulating in the plasma is capable of making its way to the target tissue, which enhances its therapeutic efficiency may minimize its unwanted adverse reactions [19,20]. Serum albumins are not only simple expanders to the plasma volume but more importantly represent the primary transporting proteins inside the blood, they are capable of binding numerous ligands including therapeutic agents [21]. A high impact on the pharmacological profiles of those therapeutic agents is pertained on their binding to serum albumin [22]. Thus, complete examination of the affinities of the different drugs to serum albumin is a crucial element in determining their pharmacokinetics and pharmacodynamics features. In the same context, the current study is designed to thoroughly examine the interactions of AZL, EPR and OLM to bovine serum albumin (BSA) as a representative of the serum albumin family. Extensive survey of the literature returned one published report on the binding of some ARBs including EPR and OLM with human serum albumin (HSA) [4] using docking and molecular dynamics simulation . Such study has only considered the theoretical parameters using computer-based simulation approaches and not systematically investigating the experimental procedure to estimate the different binding parameters. Therefore, the present work is devoted to utilize a set of spectroscopic procedure supplemented by molecular modelling studies to deeply explore the affinities of such ARBs to BSA and systematically define the binding-associated characteristics.

2. Materials and methods

2.1. Chemicals and reagents

Azilsartan (AZL), Eprosartan (EPR) and Olmesartan (OLM) reference standards were purchased from MedChem Express (NJ, USA). Bovine serum albumin (BSA) was procured from Techno Pharmchem (Haryana, India). All other reagents and chemicals were procured from Sigma-Aldrich Co. (St. Louis, MO, USA). The Millipore Milli-Q® UF-Plus purification system (Millipore, MA, USA) was used to collect the needed Ultra-pure water to carry out the study.

2.2. Sample preparation

1.0 mM individual methanolic solutions of AZL, EPR and OLM were prepared with subsequent dilution with phosphate buffered saline pH~7.4 (1X PBS buffer) to get different working solutions of AZL, EPR and OLM. In addition, a 1.5 μM solution of BSA was obtained by sequential dilution of its 15 μM solution in PBS.

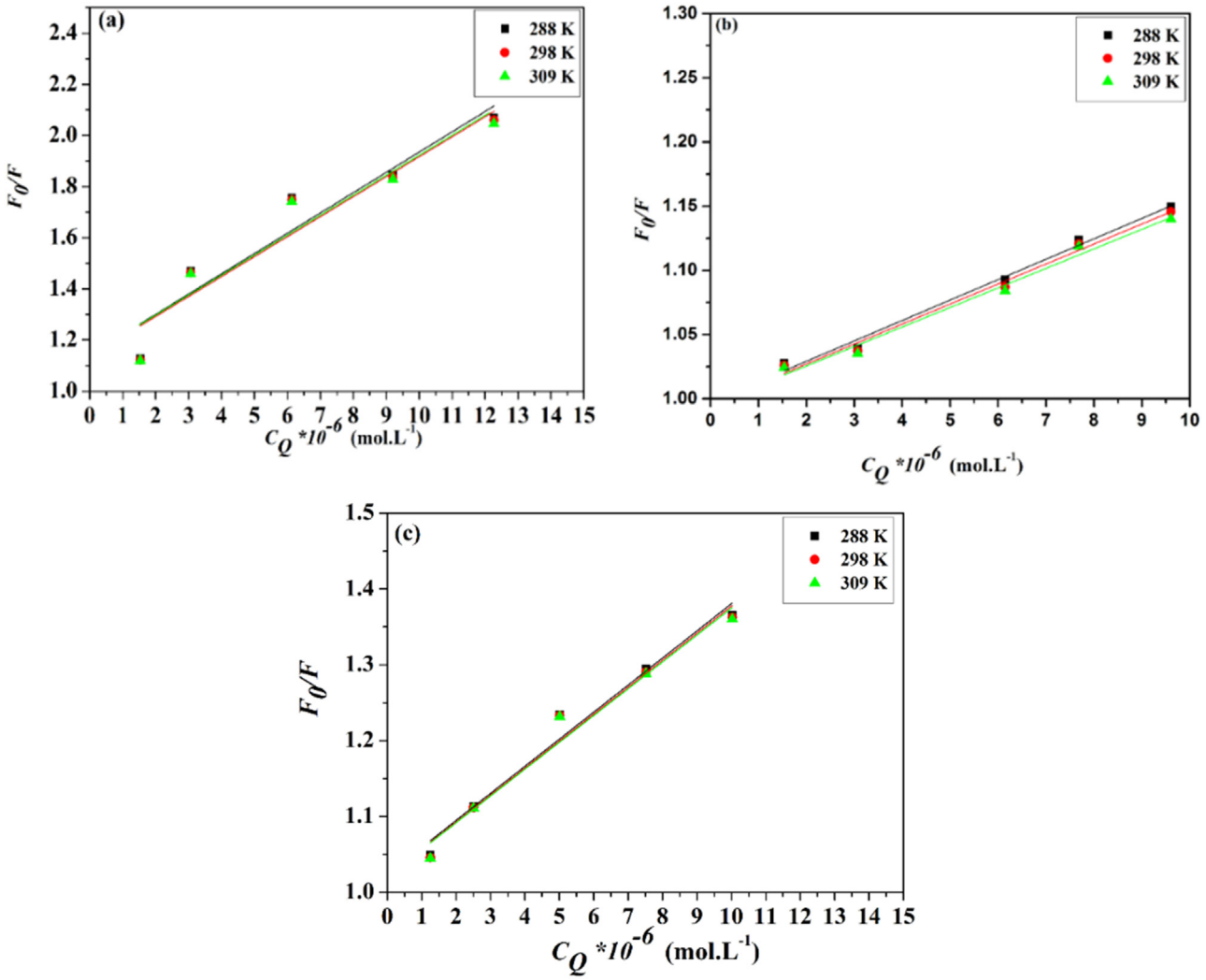

Fig. 4. Plots of the data obtained from **(a)** AZL/BSA **(b)** EPR/BSA and **(c)** OLM/BSA systems using the Stern–Volmer relation.

Table 1
The determined parameters from the Stern-Volmer and the double-log binding relations for AZL, EPR and OLM upon their binding to BSA.

	Temperature (T) (K)	Stern-Volmer parameters			Double-log binding parameters		
		$K_{SV} \times 10^4$ (L mol^{-1})	$K_q \times 10^{13}$ (L mol^{-1} s^{-1})	r^2	$K \times 10^4$ (L mol^{-1})	n^*	r^2
AZL	288	7.93 ± 0.30	2.94	0.9565	7.92 ± 0.17	0.98 ± 0.08	0.9514
	298	7.90 ± 0.24	2.93	0.9610	7.78 ± 0.12	0.97 ± 0.08	0.9981
	309	7.89 ± 0.33	2.89	0.9556	7.75 ± 0.15	0.95 ± 0.07	0.9910
EPR	288	1.59 ± 0.09	0.59	0.9950	1.59 ± 0.19	1.01 ± 0.09	0.9856
	298	1.56 ± 0.10	0.56	0.9939	1.24 ± 0.15	0.99 ± 0.09	0.9860
	309	1.52 ± 0.11	0.56	0.9929	1.06 ± 0.14	0.97 ± 0.09	0.9859
OLM	288	3.57 ± 0.32	1.32	0.9878	3.79 ± 0.07	0.99 ± 0.08	0.9902
	298	3.55 ± 0.34	1.32	0.9867	3.53 ± 0.15	0.99 ± 0.07	0.9906
	309	3.53 ± 0.34	1.31	0.9866	3.13 ± 0.18	0.96 ± 0.06	0.9927

2.3. Spectroscopic studies

2.3.1. Fluorescence measurements

Jasco FP-8200 (Jasco Int. Co. Ltd. Tokyo, Japan) was utilized to assess fluorescence (emission, synchronous and three dimensional) using 1 cm quartz cuvette. Values for the λ_{em} was set in the range of 290–500 nm succeeding the excitation at λ_{ex} 280 nm and the excitation and emission slit widths were adjusted to 5 nm for spectral examinations. Standard measurements of the emission spectra of individual ligands alone were carried out using concentrations of 6.0, 6.0 and 5.0 μM of AZL, EPR and OLM respectively. The quenching effects of AZL, EPR and OLM on the BSA were observed through scoring emission and synchronous fluorescence at three different temperatures (288, 298 and 309 K). 1.5, 3.0, 6.0, 9.0 and 12 μM concentrations of AZL, 1.5, 3.0, 6.0, 8.0 and 10 μM concentrations of EPR and 1.25, 2.5, 5.0, 7.5 and 10 μM concentrations of OLM were mixed with equal volumes of 1.5 μM BSA to determine emission and synchronous spectra. The wavelength intervals (Δλ) were set to 15 and 60 nm to monitor the synchronous fluorescence of AZL, EPR and OLM-BSA systems. Meanwhile, a 1.5 μM solution of BSA was utilized to observe the 3D spectra in absence of the

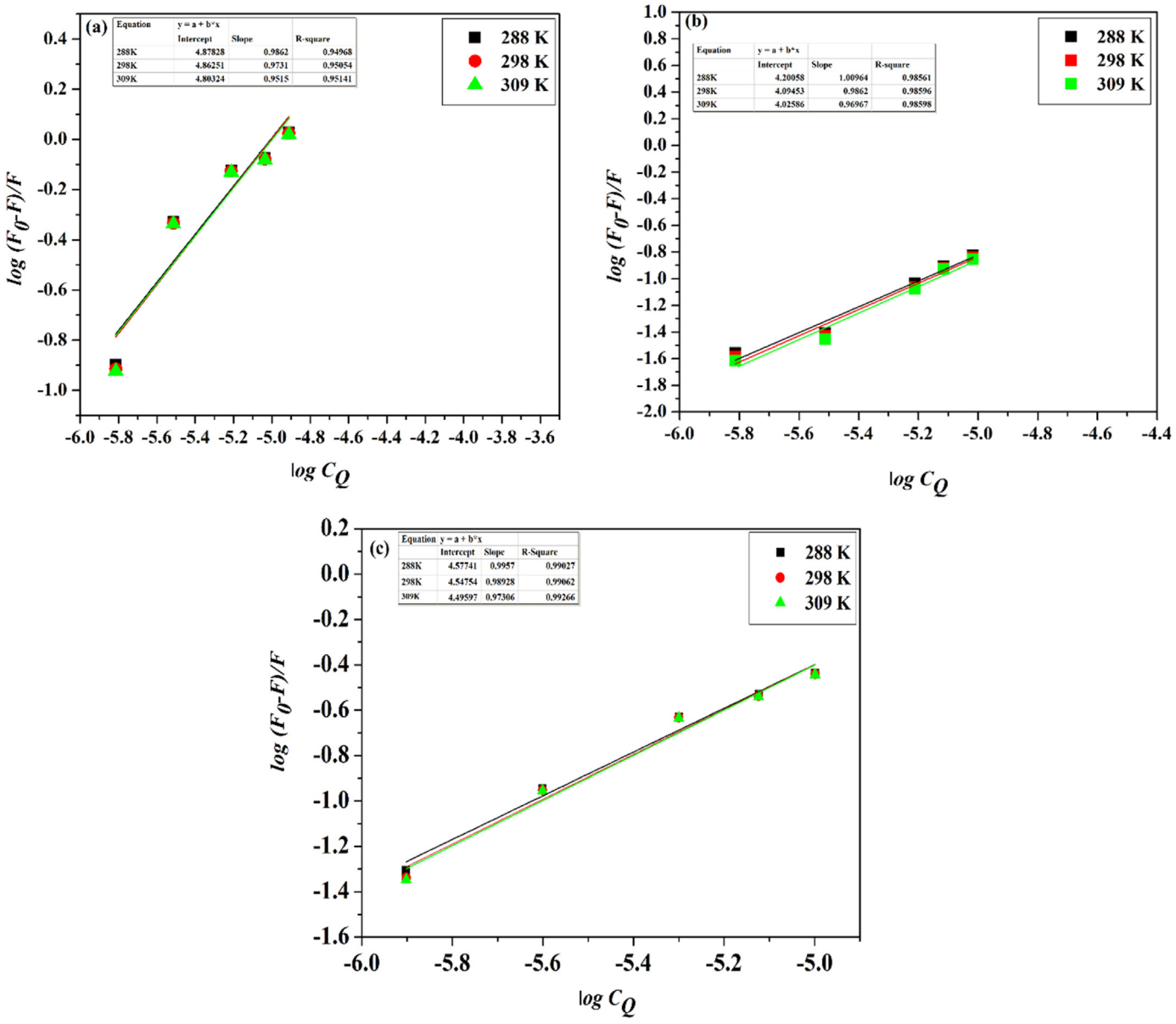

Fig. 5. Plots representing **(a)** AZL-BSA and **(b)** EPR-BSA and **(c)** OLM-BSA systems as constructed using the double-log equation.

Table 2
Summarized values of the thermodynamic parameters for AZL-BSA, EPR-BSA and OLM-BSA.

	Temp. (T) *(K)*	ΔG°(kJ mol^{-1})	ΔH° (kJ mol^{-1})	ΔS° (J mol^{-1} K^{-1})
AZL	288	− 27.00 ± 0.09	− 0.74 ± 0.05	91.18 ± 0.17
	298	− 27.91 ± 0.09		
	309	− 28.92 ± 0.10		
EPR	288	− 23.06 ± 0.05	− 12.78 ± 1.19	35.72 ± 3.99
	298	− 23.42 ± 0.01		
	309	− 23.82 ± 0.03		
OLM	288	− 25.26 ± 0.07	− 6.77 ± 0.35	64.23 ± 1.19
	298	− 25.91 ± 0.08		
	309	− 26.62 ± 0.20		

All values are average of three determinations.

examined ligands as well as in their presence, AZL (3.0 μM), EPR (3.0 μM) and OLM (2.5 μM). The fluorescence intensity was scanned and recorded in the excitation and emission ranges of 210–350 nm and 240–610 nm, respectively, after adjusting the 3D experimental parameters. Furthermore, Eq. (1) [23,24] was used to exclude the inner filter effect

$$F_{cor=F_{obs}\times e^{(A_{ex}+A_{em})/2}} \quad (1)$$

Where both corrected and observed fluorescence emission intensities were expressed as F_{cor} and F_{obs}, respectively. While, A_{ex} and A_{em} represent the analytes' absorbance values at the excitation and emission wavelengths, respectively.

Additionally, fluorescence emission measurements of the previously reported BSA site markers viz. phenylbutazone (PHB) and ibuprofen (IBP) were used to recognize the binding site(s) on the protein for each tested ligand. Both PHB and IBP were previously crystallized with the human serum albumin (HSA) and they bind to Sudlow sites I and II, respectively. 1.5 μM solutions of these site markers and BSA were prepared as described earlier for the tested ligands, whereas solutions of the studied ARBs were prepared identically as for the steady state fluorescence emission measurements. Site markers solutions were mixed with BSA followed by titration with OLM, AZL, and EPR and subsequently fluorescence spectra were recorded.

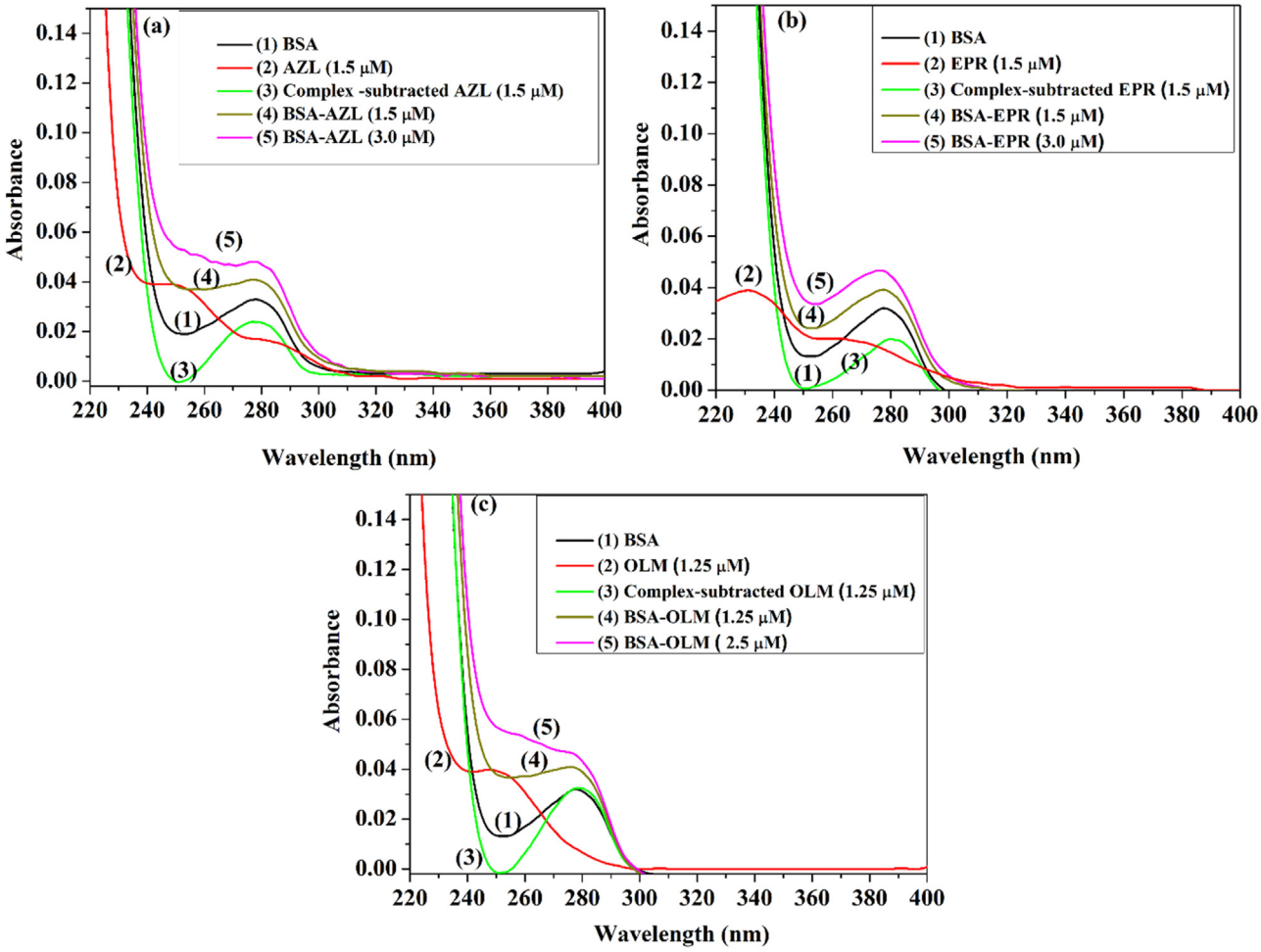

Fig. 6. Plots representing the recorded UV spectra for the binding of **(a)** AZL **(b)** EPR and **(c)** OLM with BSA.

2.3.2. *UV–Vis studies*

Steady-state studies of protein-ligand interactions are frequently performed with the aid of Ultraviolet-visible (UV–vis) absorption spectroscopy [25]. Conformational changes of the protein can be monitored through UV–vis spectral examinations. UV-1800 Schimadzu™ double beam UV–vis spectrophotometer (Schimadzu Corporation, Tokyo, Japan) was used to estimate AZL, EPR and OLM-BSA complexes at 220–450 nm. AZL (1.5 and 3.0 μM), EPR (1.5 and 3.0 μM) and OLM (1.25, 2.5 μM) concentrations were used to estimate ligands alone and after their binding with fixed concentration of BSA (1.5 μM).

2.4. *Molecular docking*

The 3D structures of AZL, EPR and OLM, sketched using ChemDraw® Ultra 14.0, and the 3D structure of human serum albumin complexed with phenylbutazone (PDB code 2BXC) [26] were used to carry out molecular simulation studies. Molecular Operating Environment software package (MOE® 2014) was used for structure optimization and energy minimization of the ligands as well as for pre-optimization of the BSA structure regarding heteroatoms and water molecules removal and addition of hydrogen atoms. London dG and GBVI/WSA dG functions implemented in the MOE® software were utilized for scoring and re-scoring of the orientations of the docked analytes inside the BSA binding pocket. Based on their theoretical pKa values at the experimental pH of 7.4 [27], the ionized structures of AZL, EPR and OLM were used for the docking study to simulate the actual working solutions. The docked conformations of AZL, EPR and OLM were assessed according to their scores and root mean square deviation (RMSD) values.

3. Results and discussion

3.1. *Steady-state fluorescence measurements*

Spectrofluorimetric monitoring of the intrinsic fluorescence quenching of a macromolecule induced by its binding to a certain ligand can provide enormous amount of information. Such quenching can be a consequence of a dynamic process viz. molecular diffusion in solution or a static process upon forming a complex between the drug and the macromolecule. In both cases, temperature escalation can either result in an enhanced or reduced binding constant in static or dynamic quenching, respectively [28]. Hence, in this study binding of the studied ARBs resulted in a concentration-dependent decline in the fluorescence intensity of BSA as shown in Fig. 2b-c with no effect on peak shape or position in case of EPR and OLM. Whilst producing a bathochromic shift with AZL binding (Fig. 2a) which could be a result of a conformational change in the BSA or fluorescence emitted by the unbound AZL (Fig. 3a). Concomitantly, fluorescence spectra of the standard EPR and OLM solutions showed negligible fluorescence response at the investigated excitation and emission wavelengths (Fig. 3b-

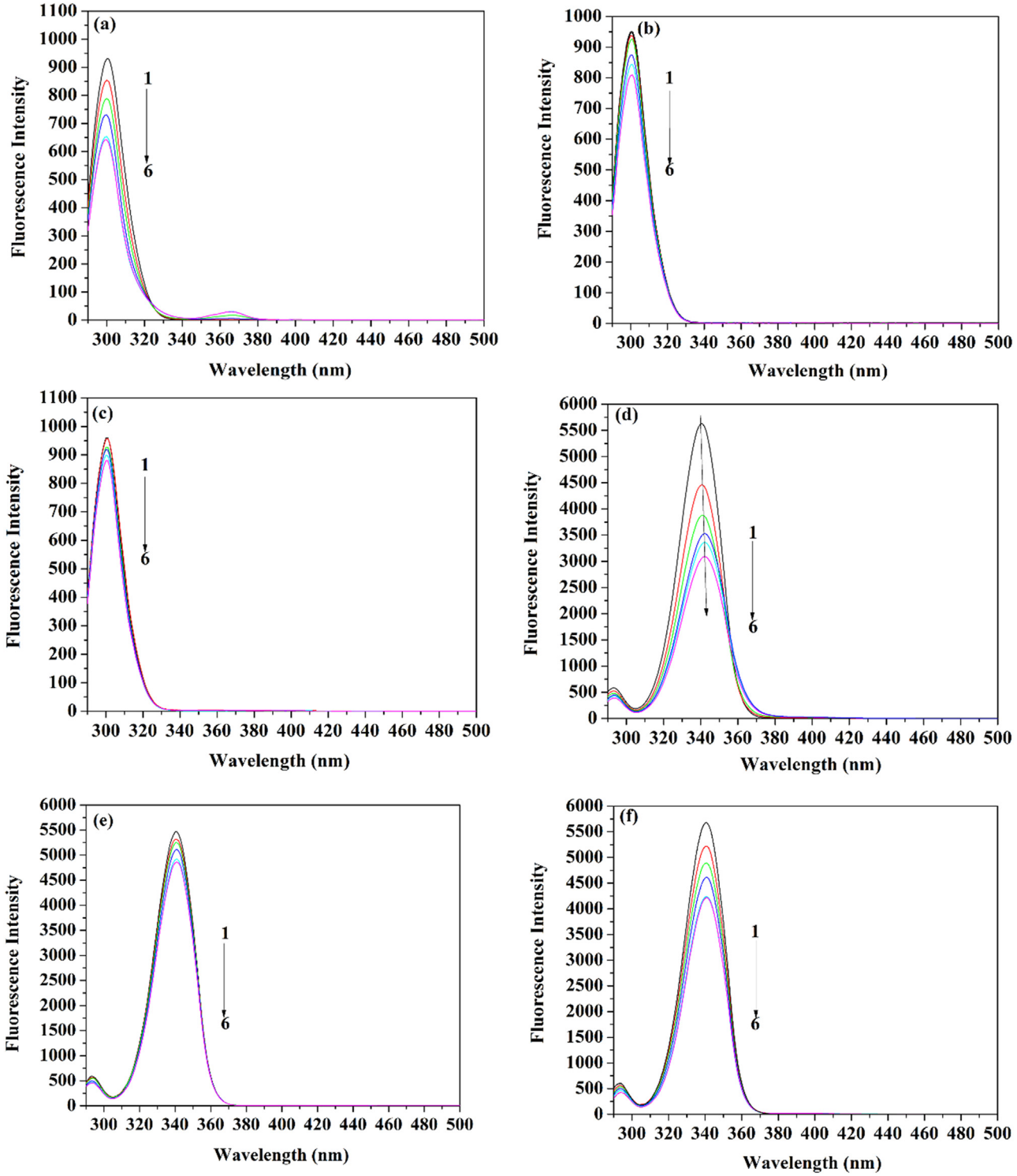

Fig. 7. Overlaid synchronous spectra of BSA (1.5 μM) at Δλ = 15 nm, upon interacting with **(a)** AZL (numbers 1–6 correspond to 0–35.5 μM) **(b)** EPR (numbers 1–6 correspond to 0–34.7 μM) **(c)** OLM (numbers 1–6 correspond to 0–34.7 μM) and at Δλ = 60 nm for **(d)** AZL **(e)** EPR **(f)** OLM (at the same concentrations).

Table 3
Features of the BSA binding to the studied ARBs as obtained by 3D fluorescence.

	BSA		AZL-BSA		EPR-BSA		OLM-BSA	
	1st Peak	2nd Peak	1st Peak	2nd Peak	1st Peak	2nd Peak	1st Peak	2nd Peak
Peak position (λex/λem) (nm)	226/342	280/342	226/342	280/342	226/342	280/342	226/342	280/342
Relative intensity (*IF*)	4580.56	5463.85	2779.92	3688.72	3672.79	4330.56	2492.22	4497.71
Δλ (nm)	116	62	116	62	116	62	116	62

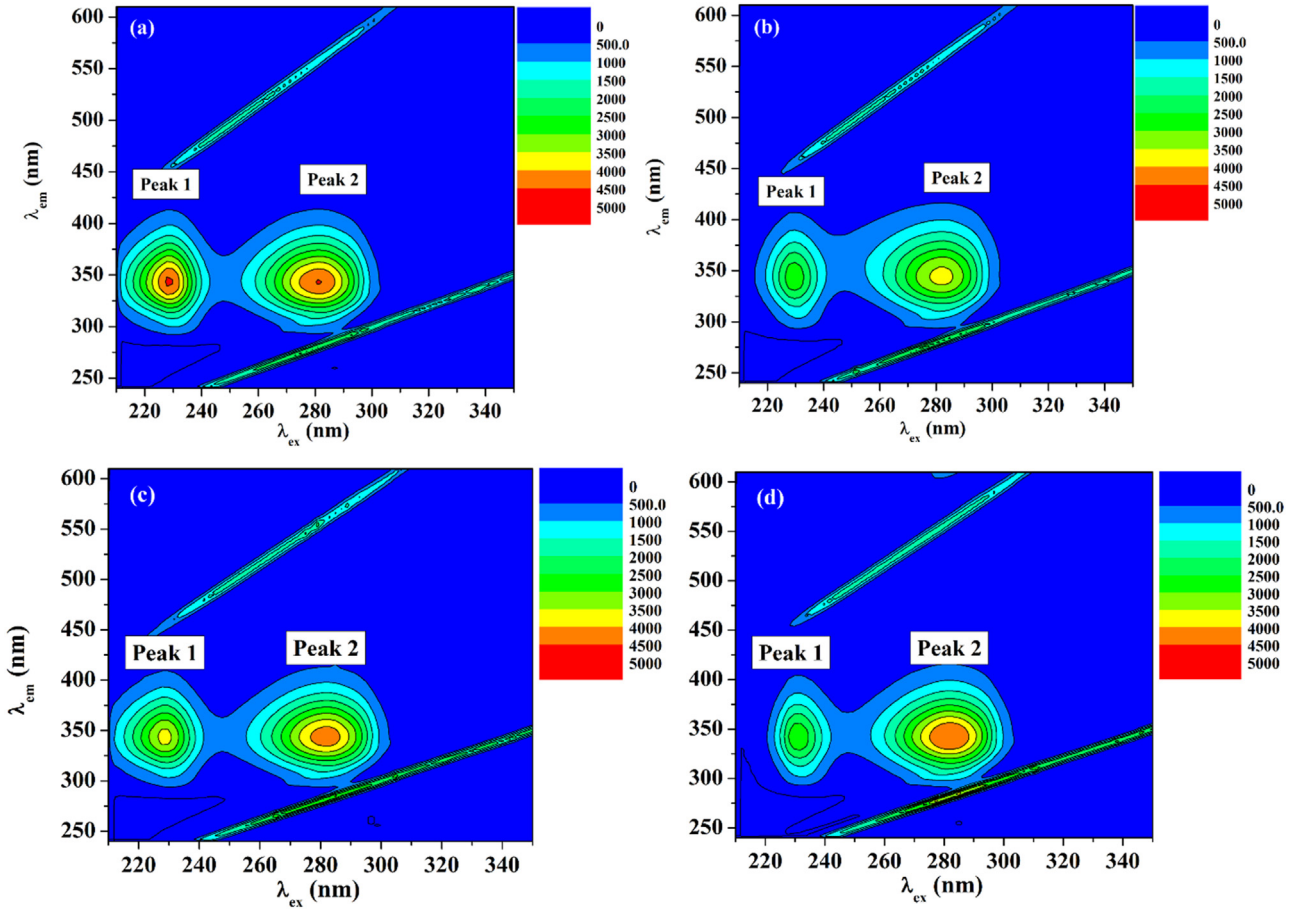

Fig. 8. 3D fluorescence of the protein (BSA) (1.5 μM) in its **(a)** unbound state, and when bound to **(b)** AZL (3.0 μM) **(c)** EPR (3.0 μM) **(d)** OLM (2.5 μM).

c). Ensued analysis of the recorded spectral information was executed using Stern–Volmer relation (Eq. (2)) to elaborate the binding characteristics involved for the studied ARBs and BSA interactions

$$F_0/F = 1+K_{SV}C_Q = 1+K_q\tau_0C_Q \quad (2)$$

$$K_q = K_{SV}/\tau_0 \quad (3)$$

Herein, F_0 and F are the determined intensities of the BSA fluorescence in absence and presence of the drug, respectively. C_Q is the drug added concentration, K_{SV} is the Stern–Volmer constant. K_q is the quenching rate constant, which can be estimated using Eq. (3) and utilizing the value for τ_0 (mean protein lifetime with no quencher) reported in the literature as $\sim 2.7 \times 10^{-9}$ s^{-1} [28]. Moreover, the temperature effect was monitored via repeated steady state fluorescence measurements at the temperatures of 288, 298 and 309 K. The observed results revealed a decrease in the Stern Volmer constant, which is in good agreement with a formation of a steady state non-fluorescent complex. Fig. 4a-c represent the plotted data at the different temperatures using the Stern–Volmer relation for the three studied systems for AZL, EPR and OLM. These plots show linear fitting of the data, which indicates static binding of the drugs to the protein. Based on the fitting results of such plots, values of K_{sv} and K_q were calculated for AZL, EPR and OLM as reported in Table 1. In view of the results listed in Table 1, those K_q values are in the 10^{13} magnitude that is higher compared to the earlier reported 2×10^{10} $L\,M^{-1}\,s^{-1}$ [29] for some quenchers with a biopolymer signifying formation of steady state complexes between BSA and AZL, EPR and OLM [30].

Further spectral analysis of the steady state fluorescence via the double-log equation (Eq. (4)) was performed to explore the equilibrium amongst bound and unbound molecules [31,32]. Subsequent plot of $\log C_Q$ versus $\log(F_0-F)/F$ (Fig. 5) was constructed at the different concentrations and a linear fit was generated, which enabled the evaluation of K the binding constant and n the number of binding sites as summarized in Table 1. Consistently, such results showed the same degree of temperature dependence as the Stern-Volmer plotted data, which is also suggestive of a complex formation between those ARBs and BSA with each drug strongly bound to one binding site on the BSA.

$$\log\left(\frac{F_0 - F}{F}\right) = \log K + n\log C_Q \quad (4)$$

Subsequent exploration of the binding mechanism and forces involved in the interactions of AZL, EPR and OLM with BSA was performed via the determination of the thermodynamic parameters e.g. free energy (ΔG∘), entropy (Δ*S*∘) enthalpy (Δ*H*∘) of such interactions. Those parameters were calculated from the obtained K values (Table 1) which was used in Eqs. (5) and (6) along with the gas constant R and the temperature T (Kelvins). Hence, constructing plots of $ln\,K$ vs. $1/T$ followed by linear fitting can result in computing values of the thermodynamics parameters (Table 2). Succeeding the estimation of such thermodynamics parameters, the binding forces involved in the formation of a ligand-macromolecule complex can be determined [33–35]. Numerous earlier reports have suggested that hydrophobic binding yields positive values of both Δ*S*∘ and Δ*H*∘, while the opposite is true for hydrogen bonding and/or van der Waals forces and finally, a negative (nearly zero) Δ*H*∘ with a positive Δ*S*∘ values reveals electrostatic forces [33–35].

$$\Delta G^\circ = -RTlnK = \Delta H^\circ - T.\Delta S^\circ \quad (5)$$

$$\ln K = -\frac{\Delta H^\circ}{RT} + \frac{\Delta S^\circ}{R} \quad (6)$$

Accordingly, the values summarized in Table 2 hypothesize the

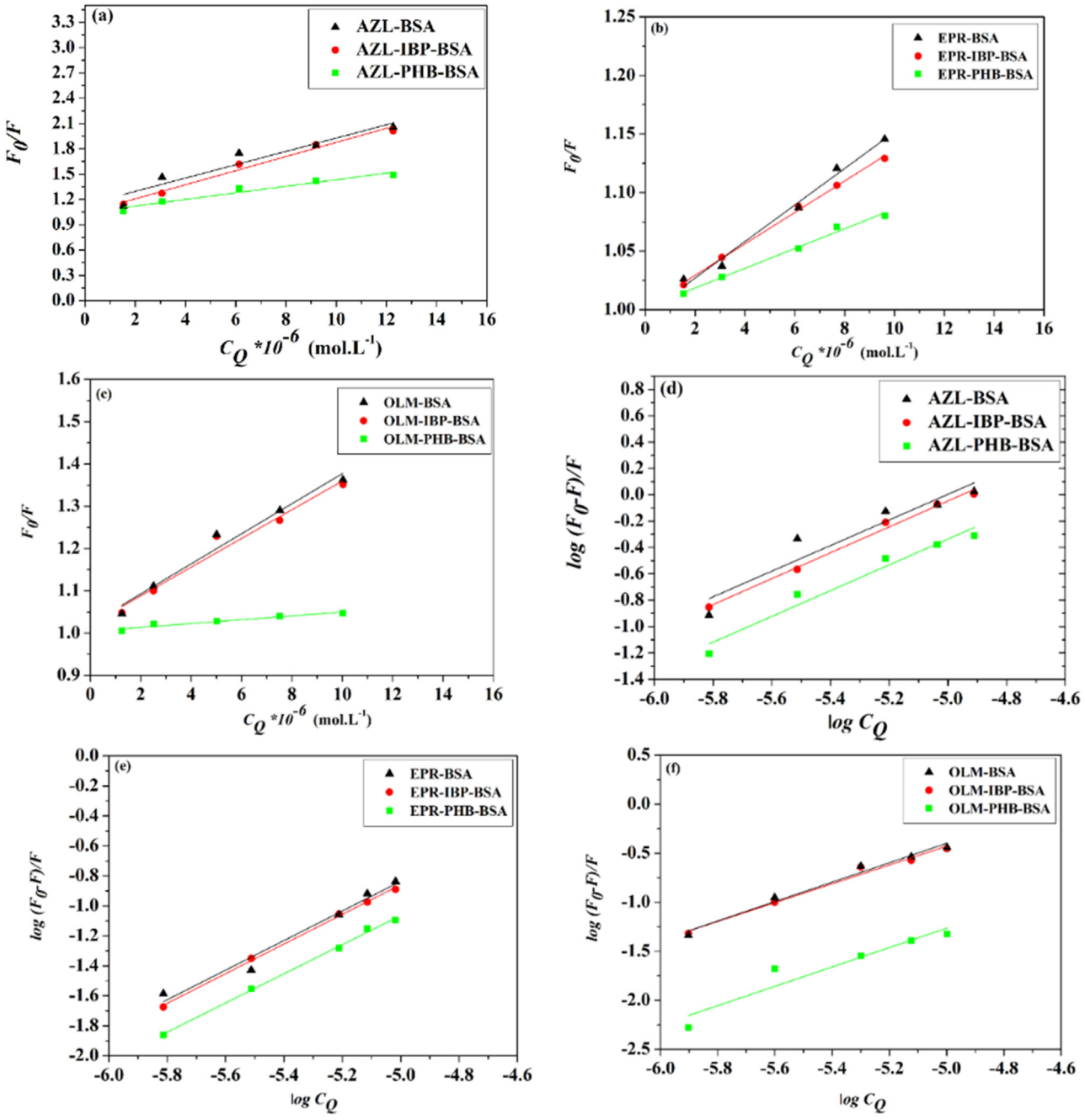

Fig. 9. Plots constructed from the Stern-Volmer and double-log relations for **(a,d)** AZL **(b,e)** EPR and **(c,f)** OLM interacrtions with the BSA bound to PHB and IBP.

occurrence of spontaneous interactions between AZL/EPR/OLM and BSA that is possibly led by electrostatic forces with the contribution of hydrogen bonding.

3.2. UV–vis spectrophotometric measurements

Observation of UV–vis spectra obtained for each ARB and BSA and their complexes (Fig. 6a-c) was executed in order to confirm complex formation and to gain further knowledge into the effect of such binding on the protein structure. Hence, it was found that static complexes were formed among the studied ARBs and BSA. Additionally, spectral subtraction of individual drugs from their complex recorded spectra unveiled noticeable changes in the peak shape and position of the BSA spectrum, which in turn enforces the formation of a static complex that affected the protein conformation.

3.3. Measurements of synchronous and 3D fluorescence

Initial description of the synchronous fluorescence was reported by Lloyd in the early 70s [36], that later provided a facile confirmatory procedure to monitor the fluorescence quenching induced by protein-ligand binding and the possible shift of the maximum λ_{em} with regard to the polarity alterations adjacent to a fluorophore. Experimentally, setting the $\Delta\lambda$ in the synchronous fluorescence measurements

Table 4
Characteristic binding parameters derived from Stern-Volmer and the double-log relations for AZL, EPR and OLM interactions with BSA-PHB and BSA-IBP systems.

	AZL		EPR		OLM	
	$K_{SV} \times 10^4$ (L.mol^{-1})	$K \times 10^4$ (L.mol^{-1})	$K_{SV} \times 10^4$ (L.mol^{-1})	$K \times 10^4$ (L.mol^{-1})	$K_{SV} \times 0^4$ (L.mol^{-1})	$K \times 10^4$ (L.mol^{-1})
Drug only	7.90 ± 0.30 (r^2 = 0.9610)	7.78 ± 0.12 (r^2 = 0.9981)	1.56 ± 0.10 (r^2 = 0.9939)	1.24 ± 0.15 (r^2 = 0.9860)	3.55 ± 0.34 (r^2 = 0.9867)	3.53 ± 0.19 (r^2 = 0.9906)
Drug-PHB (Site I)	2.00 ± 0.14 (r^2 = 0.9408)	3.57 ± 0.18 (r^2 = 0.9817)	0.84 ± 0.04 (r^2 = 0.9959)	0.62 ± 0.07 (r^2 = 0.9987)	0.45 ± 0.06 (r^2 = 0.9714)	0.47 ± 0.09 (r^2 = 0.9546)
Drug-IBP (Site II)	7.89 ± 0.28 (r^2 = 0.9820)	7.29 ± 0.15 (r^2 = 0.9965)	1.34 ± 0.05 (r^2 = 0.9987)	1.21 ± 0.12 (r^2 = 0.9992)	3.39 ± 0.35 (r^2 = 0.9843)	3.46 ± 0.27 (r^2 = 0.9922)

parameters at 15 nm or 60 nm, demonstrates the changes in polarity around the tyrosine (Tyr.) or tryptophan (Trp.) residues, respectively, in the structure of the studied protein [37,38]. The results obtained from such procedure may only show a decrease in the intensity of the fluorescence peak with no wavelength change, which in turn signifies stable non-disrupted microenvironment around the amino residue of concern. Alternatively, results may demonstrate a red shift or blue shift in the fluorescence emission wavelength which corresponds to an increased hydrophilicity or hydrophobicity, respectively surrounding such fluorophore [39,40]. In the same context, it was observed herein in Fig. 7a-f that succeeding their interactions with BSA, intrinsic fluorescence of the protein has been steadily reduced in a concentration dependent manner. Furthermore, no changes in the wavelength or peak shape were detected apart from an observed red shift in the interaction AZL with BSA when measuring at Δλ 60 nm (signifying Trp.) (Fig. 7d) which is consistent with the previous results from steady state fluorescence (Figs. 2a and 3a). The later observation may suggest a slight change in the microenvironment adjacent to the Trp. residues of the BSA leading to a less hydrophobic microenvironment.

Additionally, spectral recording of the BSA 3D fluorescence in its free unbound as well as bound states to the studied ARBs was executed with the determination of the different 3D parameters summarized in Table 3. Contour plots of the 3D fluorescence (Fig. 8a-d) disclose 2 fluorescence maxima of the protein at $\lambda_{ex}/\lambda_{em}$ of 226/342 and 280/342 which were previously reported to signify the $n \rightarrow \pi^*$ transition of the polypeptide backbone (at 226/342) and the Trp. and Tyr. residues (at 280/342) [21,41]. The two peaks have displayed decline in the fluorescence intensity induced by the binding to the studied ARBs without any observable peak shift.

3.4. Site markers competitive binding

Serum albumins are mainly constructed of three domains numbered as I, II and III with each of them features two subdomains A and B with common conformational components. BSA is privileged with two principal binding sites at which numerous ligands have been previously reported to bind, those sites are best known as Sudlow sites I and II located in subdomains IIA and IIIA, respectively [42,43]. The latter fact along with crystallization studies of various ligands showing their binding to such sites, have motivated the use of these ligands as site markers providing a straightforward protocol to explore the involved binding regions in the diverse ligand interactions. Herein in the present study phenylbutazone (PHB) and ibuprofen (IBP) were employed to label sites I and II of the BSA, respectively [44–46]. Intensity of the fluorescence emission was observed and interpreted using Stern-Volmer (Eq. (2)) and the double-log (Eq. (5)) relations and plots were generated for AZL, EPR and OLM interactions with BSA-PHB and BSA-IBP systems (Fig. 9a-g). Table 4 features the important parameters derived from those binding displacement studies, from which it can be observed that AZL , EPR and OLM have shown significant tendency towards binding Sudlow site I. This in fact was evident from the decline in both K_{sv} and K numbers as from their control (no markers) values, whilst maintaining the same values as the control in case of IBP.

3.5. Molecular docking

Subsequent computer-based docking studies were conducted to ultimately complete the picture for the AZL, EPR and OLM binding to BSA. It was then consistently determined that all the three ligands bind to site I of the BSA. Grading and ranking of the AZL, EPR and OLM conformers binding to the different binding regions of the BSA were accomplished utilizing the London dG and GBVI/WSA dG features in the MOE® software. The optimal AZL, EPR and OLM bound poses to BSA possessing the lowest ΔG values were selected (Fig. 10a-k) with those binding energies as well as other docking variables and the involved amino acid residues are all summarized in Table 5

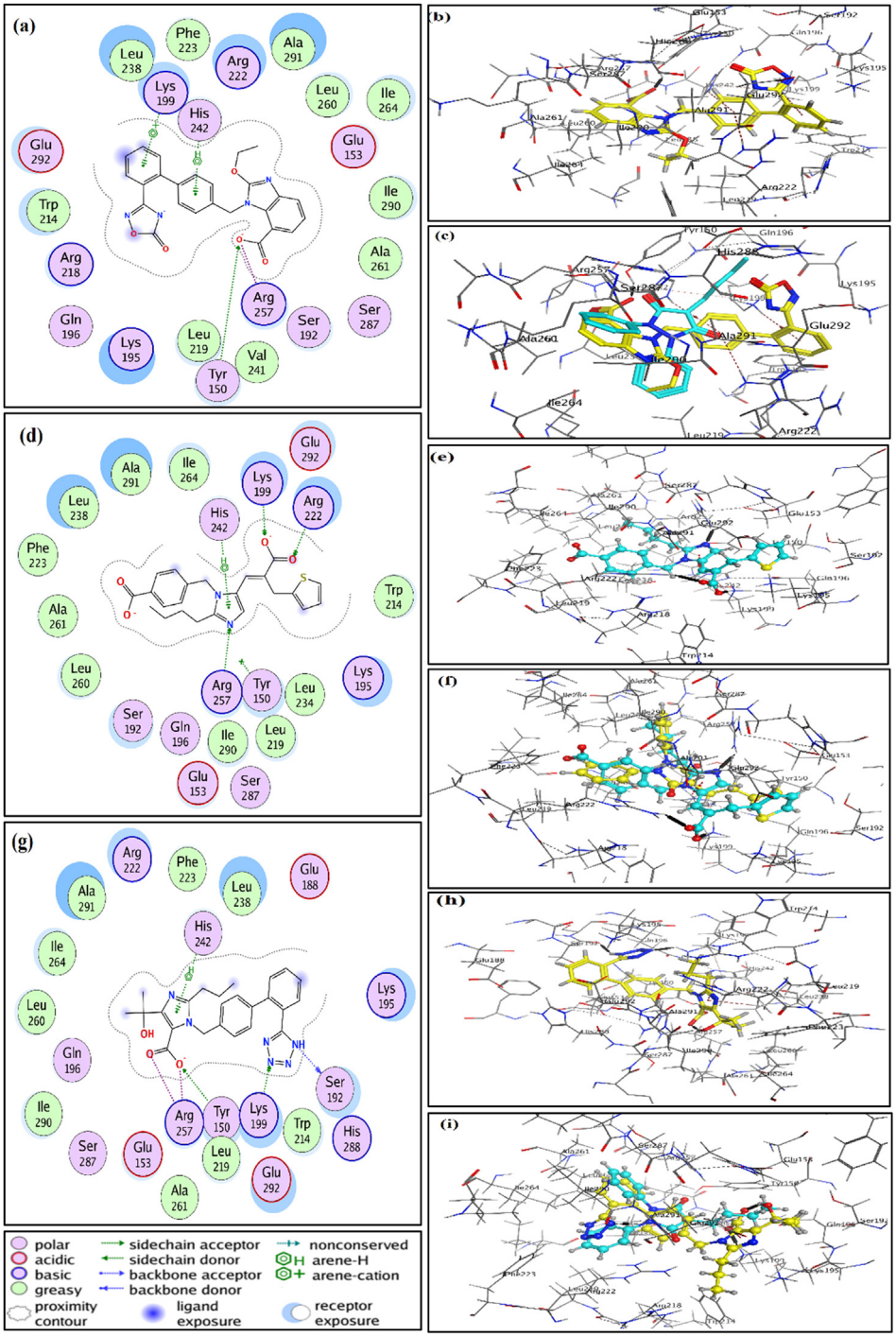

Fig. 10. Graphical illustrations demonstrating the 2D and 3D docked poses for the ionized structures of **(a-c)** AZL **(d-f)** EPR **(g-i)** OLM in site I, figures also showing the superimposed ligands with phenylbutazone (the ligand of HSA in PDB: 2BXC).

4. Conclusions

In this reported study, the interactions taking place between AZL, EPR and OLM and BSA have been characterized using spectroscopic approaches complemented with molecular docking analysis. Fluorescence quenching of the BSA was observed upon the addition of the studied ligands. Analysis of ultraviolet spectroscopic measurements presented another proof of static formation of complexes between the studied ARBs and BSA. It clearly verified such static binding by the increase in the absorption peak intensity of the complexes along with the change in the protein UV-spectrum following the subtraction of the ligand UV-spectrum from the complex. Synchronous fluorescence spectroscopy showed a red shift in the fluorescence emission peak at $\Delta\lambda$ 60 nm only in the case of AZL binding to BSA, which may infer an alteration of the microenvironment around the tryptophan residues in the BSA or may be due to the fluorescence emission of the unbound AZL

Table 5
Main features determined by molecular docking studies of AZL, EPR and OLM with Sudlow site I of the BSA.

Ligand	Amino acid residues	Interaction type	Distance (Å)	Total binding energy (kJ mol^{-1})
AZL	TYR 150	H-acceptor	2.47	− 29.77
	ARG 257	ionic	2.96	
	LYS 199	pi-cation	4.64	
	HIS 242	pi-H	4.86	
EPR	HIS 242	pi-H	4.19	− 29.58
	ARG 222	H-acceptor	2.73	
	ARG 257	H-acceptor	3	
	LYS 199	H-acceptor	2.76	
	ARG 222	ionic	3.35	
	LYS 199	ionic	3.15	
OLM	SER 192	H-donor	2.76	− 29.28
	LYS 199	H-acceptor	2.53	
	TYR 150	H-acceptor	2.68	
	ARG 257	ionic	3.85	
	ARG 257	ionic	3.09	
	ARG 257	ionic	3.35	
	ARG 257	ionic	3.15	
	HIS 242	pi-H	4.92	

. Three-dimensional fluorescence measurements displayed two fluorescence emission peaks for BSA at $\lambda_{ex}/\lambda_{em}$ of 226/342 nm and 280/342 nm with both peaks quenched with the binding of the studies ARBs. Furthermore, results obtained from competitive binding studies and molecular docking unveiled the binding of AZL, EPR and OLM to Sudlow site I of the BSA.

Competing interests

The authors declare no competing interests

Acknowledgements

The authors would like to extend their sincere appreciation to the Deanship of Scientific Research at King Saud University for its funding this Research Group No. RGP-196.

References

[1] D. Mozaffarian, E.J. Benjamin, A.S. Go, D.K. Arnett, M.J. Blaha, M. Cushman, S. de Ferranti, J.P. Despres, H.J. Fullerton, V.J. Howard, M.D. Huffman, S.E. Judd, B.M. Kissela, D.T. Lackland, J.H. Lichtman, L.D. Lisabeth, S. Liu, R.H. Mackey, D.B. Matchar, D.K. McGuire, E.R. Mohler 3rd, C.S. Moy, P. Muntner, M.E. Mussolino, K. Nasir, R.W. Neumar, G. Nichol, L. Palaniappan, D.K. Pandey, M.J. Reeves, C.J. Rodriguez, P.D. Sorlie, J. Stein, A. Towfighi, T.N. Turan, S.S. Virani, J.Z. Willey, D. Woo, R.W. Yeh, M.B. Turner, heart disease and stroke statistics–2015 update: a report from the American heart Association, Circulation 131 (2015) e29–e322.

[2] Centers for Disease Control and Prevention, High Blood Pressure Facts, Centers for Disease Control and Prevention, Atlanta, GA, 2018.

[3] National Institutes of Health National Heart Lung and Blood Institute, The Seventh Report of the Joint National Committee on Prevention, Detection, Evaluation and Treatment of High Blood Pressure., in, US Department of Health and Human Services, Bethesda, MD, USA, 2004.

[4] J. Li, X. Zhu, C. Yang, R. Shi, Characterization of the binding of angiotensin II receptor blockers to human serum albumin using docking and molecular dynamics simulation, J. Mol. Model. 16 (2010) 789–798.

[5] C. Dasgupta, L. Zhang, Angiotensin II receptors and drug discovery in cardiovascular disease, Drug Discov. Today 16 (2011) 22–34.

[6] E. Angeloni, Azilsartan medoxomil in the management of hypertension: an evidence-based review of its place in therapy, Core Evid. 11 (2016) 1–10.

[7] K. Kusumoto, H. Igata, M. Ojima, A. Tsuboi, M. Imanishi, F. Yamaguchi, H. Sakamoto, T. Kuroita, N. Kawaguchi, N. Nishigaki, H. Nagaya, Antihypertensive, insulin-sensitising and renoprotective effects of a novel, potent and long-acting angiotensin II type 1 receptor blocker, azilsartan medoxomil, in rat and dog models, Eur. J. Pharmacol. 669 (2011) 84–93.

[8] P. Sun, C. Wang, Q. Liu, Q. Meng, A. Zhang, X. Huo, H. Sun, K. Liu, OATP and MRP2-mediated hepatic uptake and biliary excretion of eprosartan in rat and human, Pharmacol. Rep. 66 (2014) 311–319.

[9] H.U. Patel, B.N. Suhagia, C.N. Patel, Simultaneous analysis of eprosartan and hydrochlorothiazide in tablets by high-performance liquid chromatography, Pharm. Methods 2 (2011) 143–147.

[10] W.B. Bollag, Regulation of aldosterone synthesis and secretion, Compr. Physiol. 4 (2014) 1017–1055.

[11] K. Koga, S.-i. Yamagishi, M. Takeuchi, Y. Inagaki, S. Amano, T. Okamoto, T. Saga, Z. Makita, M. Yoshizuka, CS-886, a new angiotensin II type 1 receptor antagonist, ameliorates glomerular anionic site loss and prevents progression of diabetic nephropathy in Otsuka Long-Evans Tokushima fatty rats, Mol. Med. 8 (2002) 591–599.

[12] L.R. Schwocho, H.N. Masonson, Pharmacokinetics of CS-866, a new angiotensin II receptor blocker, in healthy subjects, J. Clin. Pharmacol. 41 (2001) 515–527.

[13] E.M. Faed, Protein binding of drugs in plasma, interstitial fluid and tissues: effect on pharmacokinetics, Eur. J. Clin. Pharmacol. 21 (1981) 77–81.

[14] P.J. McNamara, G. Levy, M. Gibaldi, Effect of plasma protein and tissue binding on the time course of drug concentration in plasma, J. Pharmacokinet. Biopharm. 7 (1979) 195–206.

[15] S. Kageyama, B.D. Anderson, B.L. Hoesterey, H. Hayashi, Y. Kiso, K.P. Flora, H. Mitsuya, Protein binding of human immunodeficiency virus protease inhibitor KNI-272 and alteration of its in vitro antiretroviral activity in the presence of high concentrations of proteins, Antimicrob. Agents Chemother. 38 (1994) 1107–1111.

[16] D.J. Livingston, S. Pazhanisamy, D.J. Porter, J.A. Partaledis, R.D. Tung, G.R. Painter, Weak binding of VX-478 to human plasma proteins and implications for anti-human immunodeficiency virus therapy, J. Infect. Dis. 172 (1995) 1238–1245.

[17] J.A. Bilello, G.L. Drusano, D.J. Livingston, S. Pazhanisamy, J.A. Partaledis, R.D. Tung, Relevance of Plasma protein binding to antiviral activity and clinical efficacy of inhibitors of human immunodeficiency virus protease [with Reply], J. Infect. Dis. 173 (1996) 1524–1526.

[18] G.L. Trainor, The importance of plasma protein binding in drug discovery, Expert Opin. Drug Discov. 2 (2007) 51–64.

[19] M. Boffito, D.J. Back, T.F. Blaschke, M. Rowland, R.J. Bertz, J.G. Gerber, V. Miller, Protein binding in antiretroviral therapies, AIDS Res. Human. Retrovir. 19 (2003) 825–835.

[20] L.Z. Benet, I.L.O. Buxton, Pharmacokinetics: the dynamics of drug absorption, distribution, metabolism, and elimination, in: L.L. Brunton, B.A. Chabner, B.C. Knollmann (Eds.), Goodman and Gilman's the Pharmacological Basis of Therapeutics, The McGraw-Hill Companies, Inc., NY, USA, 2010, pp. 3–27.

[21] A. Sułkowska, Interaction of drugs with bovine and human serum albumin, J. Mol. Struct. 614 (2002) 227–232.

[22] J.H. Lin, D.M. Cocchetto, D.E. Duggan, Protein binding as a primary determinant of the clinical pharmacokinetic properties of non-steroidal anti-inflammatory drugs, Clin. Pharmacokinet. 12 (1987) 402–432.

[23] C. Dufour, O. Dangles, Flavonoid–serum albumin complexation: determination of binding constants and binding sites by fluorescence spectroscopy, Biochim. Biophys. Acta (BBA)-General. Subj. 1721 (2005) 164–173.

[24] J.R. Lakowicz, Principles of Fluorescence Spectroscopy, Springer Science & Business Media, 2007.

[25] K. Nienhaus, G.U. Nienhaus, Probing heme protein-ligand interactions by UV/visible absorption spectroscopy, Methods Mol. Biol. (Clifton, N.J.) 305 (2005) 215–242.

[26] A. Bujacz, K. Zielinski, B. Sekula, Structural studies of bovine, equine, and leporine serum albumin complexes with naproxen, Protein.: Struct. Funct. Bioinform. 82 (2014) 2199–2208.

[27] Chemicalize was used for prediction of pKa values, in, Chemicalize was used for prediction of pKa values, developed by ChemAxon.

[28] A.M. Alanazi, A.S. Abdelhameed, A.H. Bakheit, F.M. Almutairi, A. Alkhider, R.N. Herqash, I.A. Darwish, Unraveling the binding characteristics of the anti-HIV agents abacavir, efavirenz and emtricitabine to bovine serum albumin using spectroscopic and molecular simulation approaches, J. Mol. Liq. 251 (2018) 345–357.

[29] J.R. Lakowicz, G. Weber, Quenching of fluorescence by oxygen, Probe Struct. Fluct. Macromol. Biochem. 12 (1973) 4161–4170.

[30] W.R. Ware, Oxygen quenching of fluorescence in solution: an experimental study of the diffusion process, J. Phys. Chem. 66 (1962) 455–458.

[31] Y. Huang, Z. Zhang, D. Zhang, J. Lv, Flow-injection analysis chemiluminescence detection combined with microdialysis sampling for studying protein binding of drug, Talanta 53 (2001) 835–841.

[32] J. Liu, J.-n. Tian, J. Zhang, Z. Hu, X. Chen, Interaction of magnolol with bovine serum albumin: a fluorescence-quenching study, Anal. Bioanal. Chem. 376 (2003) 864–867.

[33] T. Forster, O. Sinanoglu, Modern Quantum Chemistry, Academic Press, New York, 1996.

[34] P.D. Ross, S. Subramanian, Thermodynamics of protein association reactions: forces contributing to stability, Biochemistry 20 (1981) 3096–3102.

[35] A.S. Abdelhameed, A.M. Alanazi, A.H. Bakheit, H.W. Darwish, H.A. Ghabbour, I.A. Darwish, Fluorescence spectroscopic and molecular docking studies of the binding interaction between the new anaplastic lymphoma kinase inhibitor crizotinib and bovine serum albumin, Spectrochim. Acta Part A: Mol. Biomol. Spectrosc. 171 (2017) 174–182.

[36] J. Lloyd, Synchronized excitation of fluorescence emission spectra, Nature 231 (1971) 64–65.

[37] J.N. Miller, Developments In clinical And biological analysis: fluorimetry and Phosphorimetry in clinical analysis, Proc. Anal. Div. Chem. Soc. 16 (1979) 56–62.

[38] S. Rubio, A. Gomez-Hens, M. Valcarcel, Analytical applications of synchronous fluorescence spectroscopy, Talanta 33 (1986) 633–640.

[39] C. Guozhen, H. Xiaozhi, Z. Zhuzi, The methods of fluorescent analysis, Science (1990).

[40] G. Chen, X. Huang, J. Xu, Z. Zheng, Z. Wang, The analytical method of fluorescence,

Science Publisher, China, 1990.
[41] A.N. Glazer, E.L. Smith, Studies on the ultraviolet difference spectra of proteins and polypeptides, J. Biol. Chem. 236 (1961) 2942–2947.
[42] G. Sudlow, D. Birkett, D. Wade, Further characterization of specific drug binding sites on human serum albumin, Mol. Pharmacol. 12 (1976) 1052–1061.
[43] S. Bi, Y. Sun, C. Qiao, H. Zhang, C. Liu, Binding of several anti-tumor drugs to bovine serum albumin: fluorescence study, J. Lumin. 129 (2009) 541–547.
[44] J. Ghuman, P.A. Zunszain, I. Petitpas, A.A. Bhattacharya, M. Otagiri, S. Curry, Structural basis of the drug-binding specificity of human serum albumin, J. Mol. Biol. 353 (2005) 38–52.
[45] Y. Ni, R. Zhu, S. Kokot, Competitive binding of small molecules with biopolymers: a fluorescence spectroscopy and chemometrics study of the interaction of aspirin and ibuprofen with BSA, Analyst 136 (2011) 4794–4801.
[46] Y. Ni, S. Su, S. Kokot, Spectrofluorimetric studies on the binding of salicylic acid to bovine serum albumin using warfarin and ibuprofen as site markers with the aid of parallel factor analysis, Anal. Chim. Acta 580 (2006) 206–215.